ISSN (Print) 1226-1750
ISSN (Online) 2233-6656
Journal of Magnetics 24(1), 81-89 (2019) https://doi.org/10.4283/JMAG.2019.24.1.081

Impact of Magnetic Field and Second-Order Slip Flow of Casson Liquid with Heat Transfer Subject to Suction/Injection and Convective Boundary Condition

Aaqib Majeed[1]*, Ahmad Zeeshan[2], Tariq Mahmood[3], Shafiq Ur Rahman[4], and Imran Khan[1]

[1]*Department of Mathematics & Statistics, Bacha Khan University, Charsada, KPK, Pakistan*
[2]*Department of Mathematics and Statistics, FBAS, IIUI, H-10, Islamabad, 44000, Pakistan*
[3]*Department of Electronics Engineering, University of Engineering and Technology Taxila sub Campus Chakwal, Pakistan*
[4]*Department of Mechatronics Engineering, University of Engineering and Technology Taxila sub Campus Chakwal, Pakistan*

(Received 17 July 2018, Received in final form 11 February 2019, Accepted 12 February 2019)

The present article is planned theoretically to throw light on non-Newtonian Casson liquid flow and heat transport analysis over an exponentially stretching sheet with second-order velocity slip condition. The analysis of magneto-hydrodynamic (MHD) is an important interdisciplinary field. One of the most imperative applications related to engineering problems is plasma confinement, liquid-metal cooling of nuclear reactors, and electromagnetic casting. The flow here is considered to be electrically conducting. The modelled equations of mass, momentum and energy transport are reduced into the nonlinear ordinary differential equations by employing a similarity approach which are then solved numerically by employing finite difference collocation process (a three-stage Lobatto IIIa scheme). The inspiration of convergence flow parameters on dimensionless velocity, temperature have been discussed graphically. The obtained results confirm that an excellent agreement is achieved for the Newtonian case with those available in the literature. Consequences establish that skin friction rises in the presence of Casson fluid parameter and the Nusselt number show enhancement for second order slip parameter.

Keywords : MHD, Casson fluid, second-order slip, suction/injection, radiation, numerically

1. Introduction

Flow and heat transfer of non-Newtonian fluids has great implication and becomes a field of active research nowadays due to its extensive application in industry, therapeutic sciences and biological progression. Such fluid occurs in industrial process for equipment dealing with molten plastics, polymeric liquids and foodstuffs. In general, non-Newtonian fluid models are more complicated, non-linear and challenging as compared to the Navier-Stoke's equations because the rheological flow parameters and viscoelastic properties appeared to make it more complex. One of the most imperative forms of non-Newtonian fluids is the Casson fluid which exhibit shear stress in Constitutive relations, an example of Casson fluid comprises honey, jelly, concentrated fruit juices, soup, tomato sauce, human blood. Boyd *et al*. [1] examined non-Newtonian oscillatory blood flow model using lattice Boltzmann method. Mustafa *et al.* [2] discussed the unsteady Casson fluid flow towards an impulsively started moving flat surface. Nadeem *et al.* [3] performed optimal series solution of steady Casson-nano fluid flow with convective boundary condition. Rana *et al.* [4] analysed the homogeneous and heterogeneous chemical reactions on the flow of mixed convection Casson fluid with partial slip. Ellahi [5] have investigated MHD and heat transport analysis of a non-Newtonian fluid with temperature dependent viscosity. Nadeem *et al.* [6] examined a Jeffrey fluid flow towards a stretching sheet under the impact of thermal radiation.

Moreover, the study of the viscous boundary layer flow and energy transport past extensible surfaces has obvious importance in industry and engineering process like the manufacture of foods, wire drawing, glass fibre, extrusion of plastic sheets, hot rolling, drawing of plastic films, fabrication of plastic and rubber sheets and various others. The insight of these applications, Wang [7] did a wonderful effort by inspecting NS equations. The phenomena of two-dimensional flow problem were firstly solved analytically by Crane [8]. He anticipated that velocity varies

*Corresponding author: Tel: +9203447825985
Fax: +9203447825984, e-mail: aaqib@bkuc.edu.pk, mjaaqib@gmail.com

linearly as the distance from the slip. Later on, Gupta *et al.* [9] elongated the problem for a moving permeable surface. The heat transfer characteristics on the continuous surface were examined by Carragher and Crane [10]. After this considerable attention, several authors did work on this problem [11-16].

The magnetic field may play an essential role in controlling momentum and heat transfers in the boundary layer flow over a stretchable surface and gained outstanding importance in the field of biomedicine including targeted drug release, asthma treatment, sterilized devices and gastric medications, the effect of synergistic in the elimination of tumours with hyperthermia. Moreover, a nuclear reactor with cooling walls, fusing metals in an electric heater, MHD generators, bearings and pumps. Pavlov [17] was the one who initially considered the transverse magnetic field and elastic deformation impact on the plane surface using boundary layer approximation. Andersson [18] obtained the exact results of steady viscous fluid flow past a stretching surface under the impact of MHD. Fang *et al.* [19] obtained a closed-form solution for magnetohydrodynamic slip flow over a stretching sheet. Turkyilmazoglu [20] examined the impact of heat and mass transfer of the MHD viscous flow under thermal slip. Bhatti *et al.* [21] investigated the MHD stagnation-point flow towards a permeable shrinking surface by employing successive linearization and Chebyshev spectral collocation scheme. Faudzi *et al.* [22] performed heat and mass transfer analysis in MHD flow over an exponentially stretching sheet in a thermally stratified medium.

Elbashbeshy [23] performed numerical simulation of viscous flow and energy transport towards an exponentially stretching sheet subject of wall mass flux. Examination of heat transport on viscoelastic fluid towards a stretchable surface was deliberated by Nadeem *et al.* [24] Mahbood *et al.* [25] studied MHD viscous flow past an exponentially stretching surface with radiation effects by applying Homotopy analysis method. Turkyilmazoglu [26] performed an analytical solution of MHD mixed convection nonlinearly deformable surface.

The understanding of the Navier boundary slip condition [27-36] has substantial importance in the designing of various microfluidic systems, red blood flow through capillaries and in many technological processes such as lubrication and permeability of microporous media, moreover slip often arises in non-homogeneous fluid, particularly slurries, suspensions, gels, foams and emulsions etc. However, for the case of non-Newtonian fluid flows boundary slip condition have more importance as compared to Newtonian fluid flow. Ariel *et al.* [37] investigated the partial velocity slip effects in viscoelastic fluid flow induced by the stretching sheet. Zeeshan *et al.* [38] analyzed the combined effect of magnetic and partial slip over a stretching/shrinking wall with a porous medium. Recently Majeed *et al.* [39] analyzed the combined influence of activation energy second-order momentum slip on MHD boundary layer flow over a stretchable surface.

The main goal of the present communication is to explore the combined impact of 2nd order slip velocity and variable magnetic field of non-Newtonian Casson fluid caused by an exponentially stretching surface. Suitable conversions are used to expose the similarity solution. Reduced system of differential equations is then solved numerically with the aid of Matlab package. The influence of Casson fluid parameter, magnetic parameter, 1st and 2nd order slip parameter, radiation parameter, suction/injection constraint on flow velocity, temperature, Nusselt number and skin-friction, are examined via graphical representations. Close surveillance of the literature reveals that no such analysis has considered before.

2. Problem Design and Formulation

Let us considered two-dimensional boundary layer incompressible flow of Casson fluid flow with second-order velocity slip towards a stretching sheet, which is electrically conducting. Heat transfer is characterized by the occurrence of thermal radiation and 2nd order velocity slip. Flow is occupied in the domain $y \geq 0$. Wall velocity of the plate is $U_w(x) = U_o e^{x/L}$, U_o is a constant. T_w is the fluid temperature at the wall which is larger than ambient temperature T_∞. The surface is heated from the bottom through convection and hot fluid of temperature T_f which offers heat transfer coefficient h_f respectively.

The rheological relation for the incompressible Casson liquid flow can be written as [5]

$$\tau_{ij} = \begin{cases} 2(\mu_B + P_y/\sqrt{2\pi})e_{ij}, & \pi > \pi_c \\ 2(\mu_B + P_y/\sqrt{2\pi_c})e_{ij}, & \pi < \pi_c \end{cases},$$

here μ_B represent plastic dynamic viscosity of Casson fluid, P_y gives the yield stress of the fluid, $\pi = e_{ij}e_{ij}$, e_{ij} indicate deformation with (i, j) the component π_c denotes a critical value. $B(x)$ is a magnetic field employed vertical to the surface as displayed in Fig. 1, the induced magnetic field is ignored owing to the lower value of the magnetic Reynolds number.

Using the boundary layer approximation theory, the flow equation of momentum and energy transfer in non-Newtonian Casson fluid are stated as [3]

$$\frac{\partial u}{\partial x} + \frac{\partial v}{\partial y} = 0, \tag{1}$$

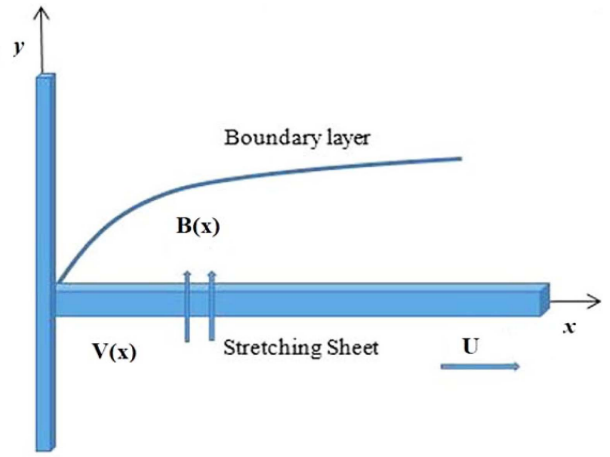

Fig. 1. (Color online) Physical sketch of the model.

$$u\frac{\partial u}{\partial x}+\mathrm{v}\frac{\partial u}{\partial y}=\nu\left(1+\frac{1}{\beta}\right)\frac{\partial^2 u}{\partial y^2}-\frac{\sigma B^2}{\rho}u\,, \tag{2}$$

$$u\frac{\partial T}{\partial x}+\mathrm{v}\frac{\partial T}{\partial y}=\alpha\frac{\partial^2 T}{\partial y^2}-\frac{1}{\rho c_p}\frac{\partial q_r}{\partial y}\,, \tag{3}$$

where u and v denote velocity components parallel to coordinate axes, $\beta=\mu_B\sqrt{2\pi_c}/p_y$ signifies the material parameter for Casson liquid, ν represent kinematic viscosity, c_p denote specific heat, ρ is fluid density, and α is thermal diffusivity,

Corresponding boundary relations are [3]

$$u=U_w(x)+U_{slip},\ \mathrm{v}=-V(x),\ -k\frac{\partial T}{\partial y}=h_1(T_f-T),\ \text{at } y=0$$
$$u=0,\ \ T=T_\infty\ \ as\ y\to\infty. \tag{4}$$

Where $B(x)=B_o e^{x/2L}$ is the variable magnetic field perpendicular to the sheet, B_o is the constant magnetic field, T is temperature, $V(x)=V_o e^{x/2L}$ is the special kind of velocity, where $V(x)<0$ signify injection and $V(x)>0$ represent suction, V_o is initial strength of suction, U_{slip} represent wall slip velocity which is specified by Wu's [27]

$$U_{slip}=\frac{2}{3}\left(\frac{3-\alpha l^3}{\alpha}-\frac{2}{3}\frac{1-l^2}{K_n}\right)\lambda\frac{\partial u}{\partial y}-\frac{1}{4}\left[l^4+\frac{2}{K_n^2}(1-l^2)\right]\lambda^2\frac{\partial^2 u}{\partial y^2}$$
$$=\mathrm{A}\frac{\partial u}{\partial y}+B\frac{\partial^2 u}{\partial y^2}. \tag{5}$$

Here K_n, α, $l=\min\left[\frac{1}{K_n},1\right]$ elucidate Knudsen number, lodging coefficients with $0\le\alpha\le1$. and $0\le l\le1$. Because the mean free path of molecular is always positive which give a negative result of B.

Now q_r is Roseland radiative heat flux, which is recognised as

$$q_r=-\frac{4\sigma}{3k^*}\frac{\partial T^4}{\partial y}, \tag{6}$$

with

$$T^4\approx 4TT_\infty^3-3T_\infty^4. \tag{7}$$

By inserting the value of Eqs. (6) and (7) into (3), we obtain

$$u\frac{\partial T}{\partial x}+\mathrm{v}\frac{\partial T}{\partial y}=\alpha\frac{\partial^2 T}{\partial y^2}+\frac{16\sigma T_\infty^3}{3\rho c_p k^*}\frac{\partial^2 T}{\partial y^2}\,. \tag{8}$$

3. Method of Solution

Now introducing the following transformation for the similarity variables [13].

$$\psi(x,y)=\sqrt{2U_0\nu L}e^{x/2L}f(\eta),\ \eta=y\sqrt{\frac{U_o}{2\nu L}}e^{x/2L},\ u=U_o e^{x/L}f'(\eta),$$
$$v=-\sqrt{\frac{U_o\nu}{2L}}e^{x/2L}\left\{f(\eta)+\eta f'(\eta)\right\},\ \theta(\eta)=\frac{T-T_\infty}{T_f-T_\infty}, \tag{9}$$

by substitution of (9) in Eqs. (2)-(3), yield the following ODE's

$$\left(1+\frac{1}{\beta}\right)f'''+ff''-2f'^2-Mf'=0, \tag{10}$$

$$\left(1+\frac{4}{3}R\right)\theta''+\mathrm{Pr}(f\theta'-f'\theta)=0, \tag{11}$$

with boundary equations

$$\begin{aligned}&f'(0)=1+\gamma f''(0)+\delta f'''(0),f(0)=s,\\&\theta'(0)=-\gamma_1(1-\theta(0)),f'(\infty)=0,\ \theta(\infty)=0.\end{aligned} \tag{12}$$

Here 1st and 2nd order slip parameters are itemized as

$$\left.\begin{aligned}\gamma=A\sqrt{\frac{U_o}{2\nu L}}e^{x/2L}=\frac{2}{3}\left(\frac{3-\alpha l^3}{\alpha}-\frac{2}{3}\frac{1-l^2}{K_n}\right)\lambda\sqrt{\frac{U_o}{2\nu L}}e^{x/2L}>0\\ \delta=B\left(\frac{U_0e^{x/L}}{2\nu L}\right)=-\frac{1}{4}\left[l^4+\frac{2}{K_n^2}\left(1-l^2\right)\right]\lambda^2\left(\frac{U_0e^{x/L}}{2\nu L}\right)<0\end{aligned}\right\}. \tag{13}$$

Now Eq. (10) and (11) to gather with Eq. (12) having a similar solution. The parameters γ and δ are a constant value and not a function of x as shown in Eq. (13). For this we set λ which is proportionate to $e^{-x/2L}$, therefore we have

$$\lambda=ce^{-x/2L}\,, \tag{14}$$

here c indicate constant of proportionality. By inserting Eq. (14) into (13), we get

$$\left.\begin{aligned}\gamma &= \frac{2}{3}\left(\frac{3-\alpha l^3}{\alpha}-\frac{2}{3}\frac{1-l^2}{K_n}\right)\sqrt{\frac{U_o}{2\nu L}}c > 0\\ \delta &= -\frac{1}{4}\left[l^4+\frac{2}{K_n^2}(1-l^2)\right]\left(\frac{U_0}{2\nu L}\right)c^2 < 0\end{aligned}\right\}. \quad (15)$$

The expression γ and δ stated Eq. (15), the solution of Eq. (10) and (11) produce similar solutions. Whereas with γ and δ signify by relations (14), and consequently generated solutions are local similar solutions. Also β is the Casson parameter, $\gamma_1 = \frac{h_1}{k}\sqrt{\frac{2\nu L}{u_0}}\frac{1}{e^{\gamma 2l}}$ is the biot number, $S = -V_o\sqrt{\frac{2L}{\nu U_o}} > 0$ (or < 0) denote the suction or injection parameter $M = \frac{2\sigma B_o^2 L}{\rho U_o}$ represents a magnetic parameter, $R = \frac{4\sigma T_\infty^3 L}{kk^*}$ indicate radiation parameter and $Pr = \frac{\nu}{\alpha}$ stands for Prandtl number,

4. Physical Quantities

The most significant measures of practical concern in the current study are Nusselt number and skin friction

$$Nu_x = \frac{q_w}{k(T_w - T_\infty)},\quad C_f = \frac{\tau_w}{\rho(U_w)^2}. \quad (16)$$

Here $\tau_w = \mu\left(1+\frac{1}{\beta}\right)\left(\frac{\partial u}{\partial y}\right)\Big|_{y=0}$, $q_w = -k\frac{\partial T}{\partial y}\Big|_{y=0}$

Using the equation (9) and (16) we have

$$\sqrt{\frac{2L}{x}}\,\mathrm{Re}_x^{1/2}\,C_f = \left(1+\frac{1}{\beta}\right)f''(0),\ \sqrt{\frac{2L}{x}}Nu/\mathrm{Re}_x^{1/2} = -\theta'(0), \quad (17)$$

here $\mathrm{Re}_x = \frac{U_w x}{\nu}$ describes local Reynolds number.

5. Numerical Results and Discussion

The set of a non-linear system of ODE's (10) and (11) along with appropriate boundary functions (12) was determined numerically by utilizing the Matlab software build in function bvp4c for various values of flow parameters. This software performs higher order finite difference method that usages collocation method which involves three-stage Lobatto IIIa scheme with fourth-order accuracy (see Shampine *et al.* [40] for more details). To recognize the behaviour of velocity, temperature, skin friction and Nusslet number under the influence of various convergence flow parameters which are elaborated through graphically. In command to justify the validity of the present scheme, the present numerical results of Nussult number for the Newtonian case are compared with Ishak [15] and Mahoob [21], which are displayed in Table 1. The outcomes reveal a good agreement and show the accuracy of our method.

The impact of Casson fluid parameter on dimensionless velocity and temperature profiles are illustrated in Fig. 2 and 3. From the sketch, we established that fluid velocity reduces expressively with increasing of Casson parameter. Because plastic dynamic viscosity increases due to an increase in β, so there exit a resistive force in fluid motion.

Table 1. Comparison of the value of Nusselt number for R, M, Pr when $\gamma = \delta = N = \lambda = \beta = \gamma_1 = 0$.

$-\theta'(0)$						
Present results						
M	R	Pr	For non-Newtonian case $\beta = \infty, \gamma_1 = 0.1$	For Newtonian case $\gamma = \delta = N = \lambda = \beta = \gamma_1 = 0$	Ishak [15]	Mabood *et al.* [25]
0	0	1	0.090519	0.954783	0.9548	0.95478
		2	0.093637	1.471460		1.47151
		3	0.094921	1.869073	1.8691	1.86909
		4	0.095661	2.204512	-	2.50012
		5	0.096154	2.500131	2.5001	-
		10	0.097341	3.660371	3.6604	3.66039
0	1	1	0.084171	0.531730		0.53121
1	0		0.089595	0.861109		0.86113
0	0.5	2	0.091479	1.073519	1.0735	1.07352
		3	0.093247	1.380752	1.3807	1.38075
		4	0.094254	1.640265	-	-
		5	0.094921	1.869073	-	-
1	1	1	0.081922	0.450571	0.450571	0.450571

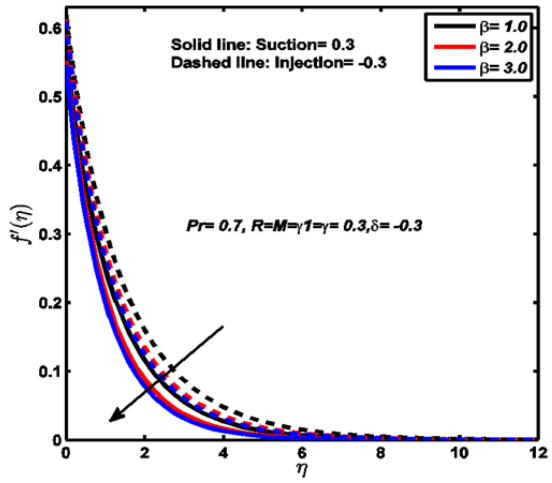

Fig. 2. (Color online) Influence of Casson fluid parameter on $f'(\eta)$.

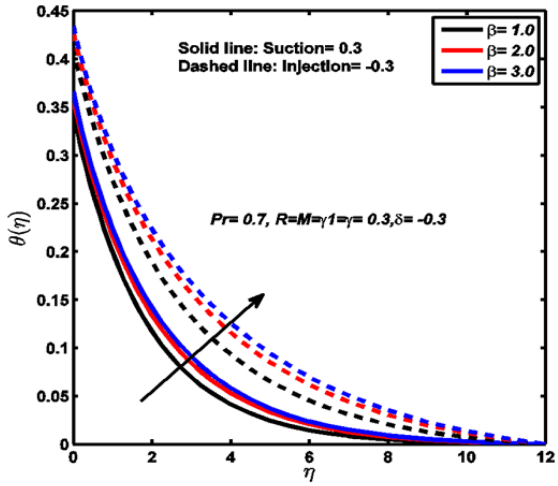

Fig. 3. (Color online) Influence of Casson fluid parameter on $\theta(\eta)$.

So the field velocity and corresponding boundary layer thickness diminish for larger Casson fluid parameter. Also noted that fluid velocity for suction (s = 0.3) is much more suppressed rather than injection (s = –0.3). The effects of Casson fluid parameter on temperature are shown in Fig. 3 which is increasing the function of β. Therefore, owing to an escalation in elasticity, the boundary layer thickness for energy increases.

Figure 4 and 5 are an outline to see the behaviour of magnetic parameter M on dimensionless velocity and temperature profiles. Results profound that, fluid velocity reduces whereas the temperature increases for the higher value of M. Physically when the magnetic field applied normal to the flow strengthen the resistive force called Lorentz force. When magnetic parameter M increase, this force increases which act in the reverse direction of flow and it has an ability to reduce the fluid velocity and corre-

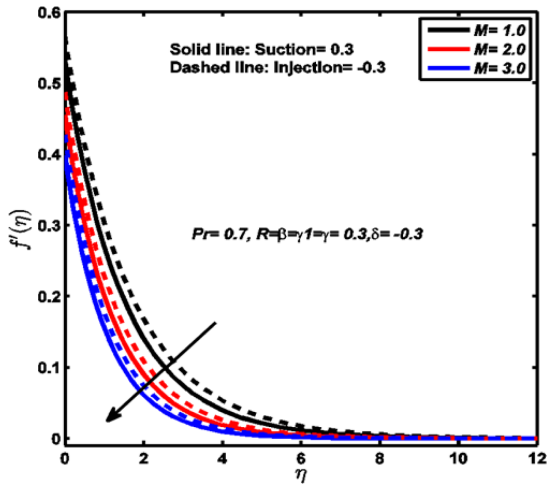

Fig. 4. (Color online) Influence of magnetic parameter on the velocity profile $f'(\eta)$.

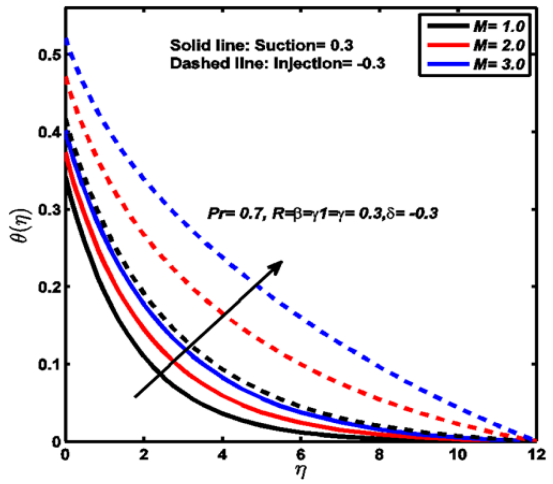

Fig. 5. (Color online) Influence of magnetic parameter on temperature profile $\theta(\eta)$.

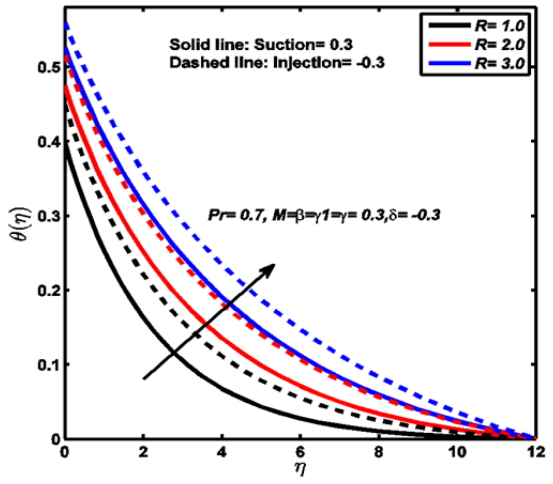

Fig. 6. (Color online) Influence of radiation parameter on temperature profile $\theta(\eta)$.

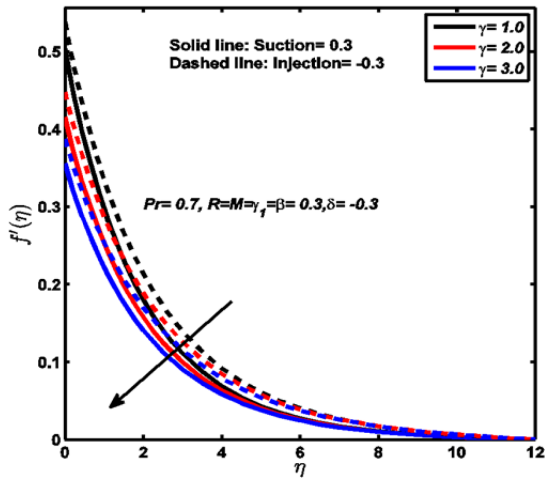

Fig. 7. (Color online) Influence of 1st order slip parameter on the velocity profile $f'(\eta)$.

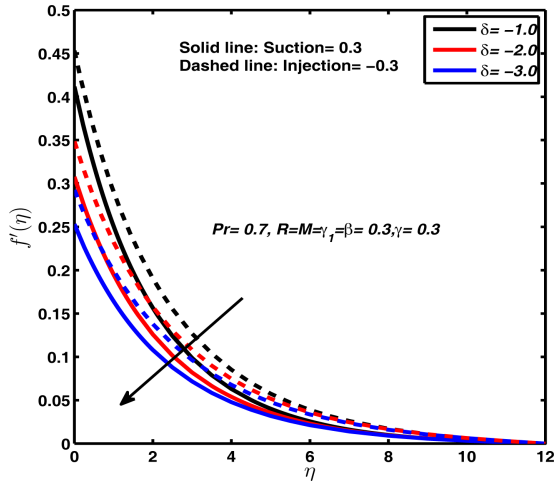

Fig. 9. (Color online) Influence of 2nd order slip parameter on velocity profile $f'(\eta)$.

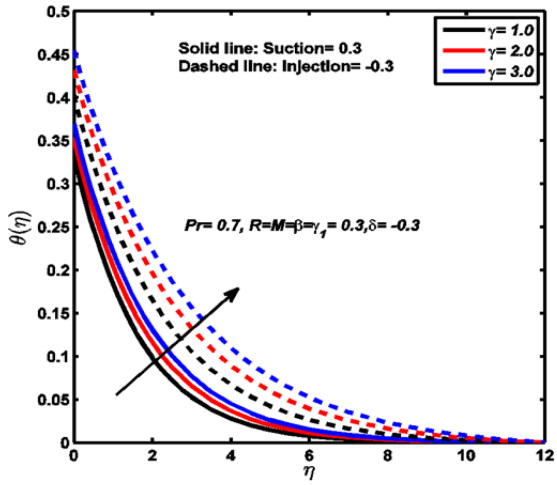

Fig. 8. (Color online) Influence of 1st order slip parameter on temperature profile $\theta(\eta)$.

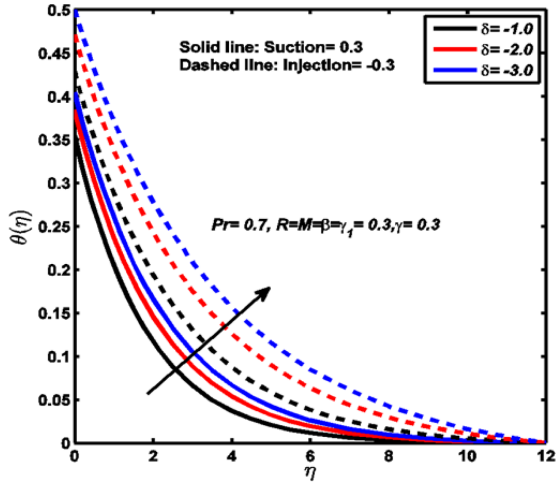

Fig. 10. (Color online) Influence of 2nd order slip parameter on temperature profile $\theta(\eta)$.

sponding boundary layer thickness. Furthermore, this force enriches the thickness of the thermal boundary layer. Also observed that fluid velocity and temperature are more noticeable for the case of injection (s = –0.3) than suction (s = 0.3). The behaviour of radiation parameter R on temperature field is demonstrated in Fig. 6. It is interesting to illustrate that the temperature of the fluid increased by raising the radiative parameter because additional heat is transported to the fluid for a large value of radiation parameter. Figs. 7 and 8 designate the impact of 1st order slip γ on velocity and temperature distributions. Graphs elaborate that velocity increases with the increasing γ. This is because of the fact under slip condition, stretching and fluid velocity near the surface are not equal. By increase γ, slip velocity speeding up and therefore fluid velocity reduces because, in the presence of slip, the pulling of stretching surface only conveyed partly to the fluid. On the other end fluid temperature enhanced against 1st order slip as clarified in Fig. 8.

Figures 9 represents the influence of the 2nd order slip parameter δ on temperature and velocityfields. It is fascinating to observe that the velocity profile gradually slow down with the rise of the absolute value of 2nd order slip parameter whereas a substantial decrement is noted in temperature. Similarly, it is also charming to comprehend that the boundary layer becomes denser for the lowest absolute value of the 2nd order slip parameter, which accelerates the size ofthe energy boundary layer as perceived in Fig. 10. The Outcome of the Biot number γ_1 on dimensionless temperature distribution describes in Fig. 11. It is witnessed that fluid temperature boost up for a large value of γ_1. Because of the fact that heat transfer coefficient involves in the thermal Biot number. So heat transmission coefficient enhances for the higher value of

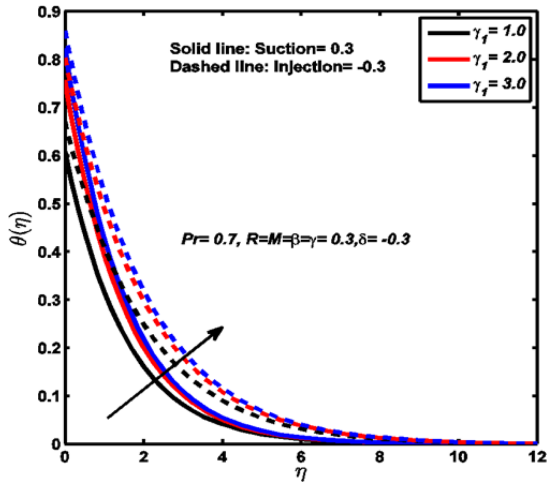

Fig. 11. (Color online) Influence of Biot number on temperature profile $\theta(\eta)$.

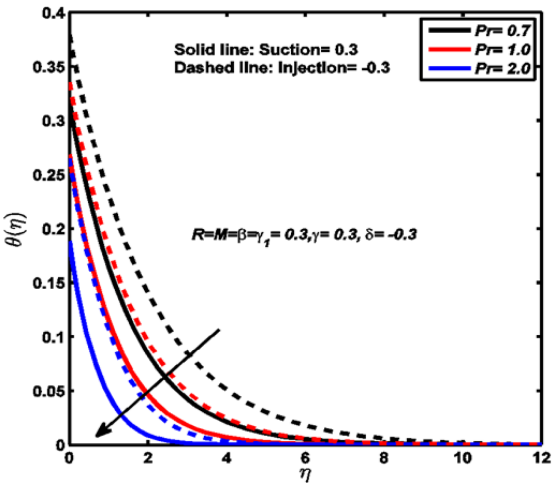

Fig. 12. (Color online) Influence of Prandtl number on temperature profile $\theta(\eta)$.

Biot number.

The impact of Prandtl number Pr is exhibited in the presence of suction and injection as illustrated in Fig. 12. Fallouts show that temperature with increasing Pr. From a physical point of view, for a small value of Pr having huge thermal diffusivity compared to the momentum diffusivity. Fluid with higher Prandtl number having a lower thermal conductivity which caused the decrement of the thickness of the energy boundary layer because it is capable to enhance the cooling rate in conducting flows.

Figures 14-17 examined the deviation of skin friction, the heat transfer rate for several values of β, s, δ, M, and γ_1. From Fig. 14 it is found that increasing values of s causes reduction in the wall shear stress whereas for the higher value of β, enhances the friction factor. Also noticed that skin friction is negative. Practically, the negative sign

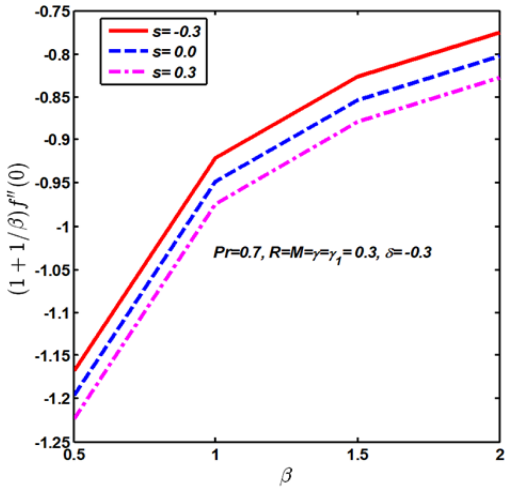

Fig. 13. (Color online) Variation of skin friction coefficient for different values of β and s.

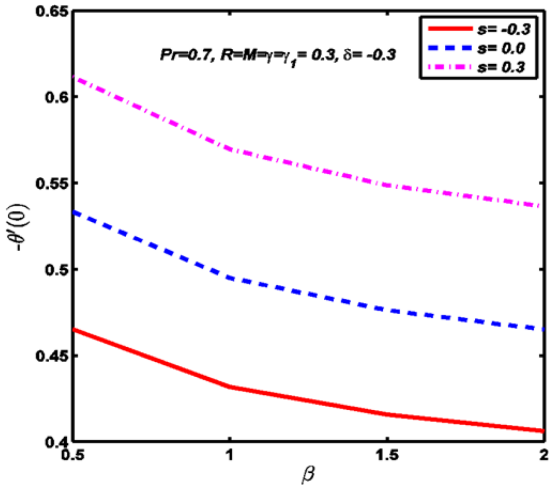

Fig. 14. (Color online) Variation of Nusselt number for different values of β and s.

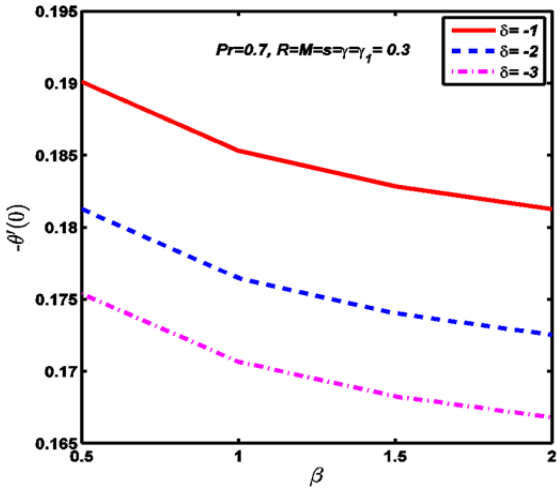

Fig. 15. (Color online) Variation of Nusselt number for different values of β and δ.

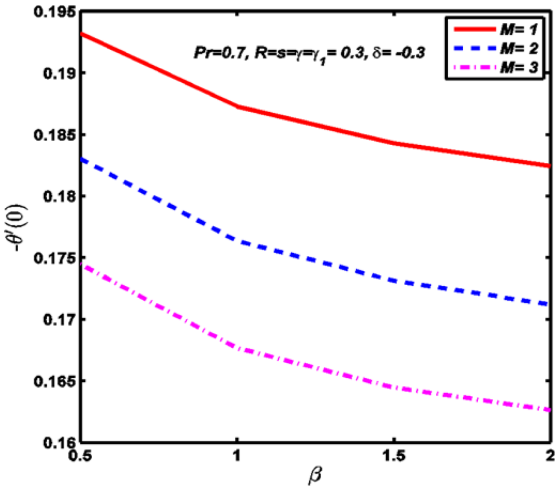

Fig. 16. (Color online) Variation of Nusselt number for different values β and M.

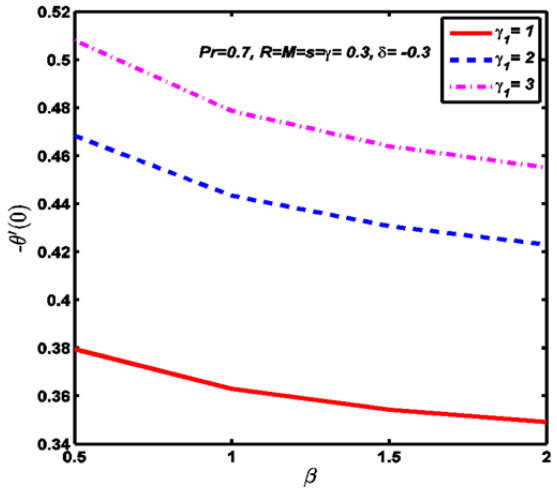

Fig. 17. (Color online) Variation of Nusselt number for different values of β and γ_1.

of $f''(0)$ indicates that wall employ drag force on the liquid whereas plus sign shows the reverse. Fig. 15 and 16 illustrate the deviation ofNusselt number for β, $s$and γ_1. From figures, it is found that Nusselt number enhances s, and γ_1 whereas opposite behaviour is noted for β. Fig. 17 offer the deviation of Nusselt number for δ and M. From this it is noticeable that heat transfer rate decreases for δ and M.

6. Final Remarks

The current study investigates the combined impact of MHD 2nd order slip of Casson fluid flow towards a stretchable surface subject to convective boundary condition. The main findings of our analysis are:

- Nusselt number is reduced against the 2nd order velocity slip parameter while opposite behaviour is observed for γ_1
- Skin friction increases with the increase in the Casson parameter
- Fluid velocity and corresponding boundary layer thickness decline for a large value of Casson parameter while the inverse trend in noted for temperature profile.
- Fluid temperature accelerates for a large value of the radiation parameter. This phenomenon occurred due to high effective thermal diffusivity.
- Temperature profile enhances for higher valued of 1st order slip parameter.
- Fluid velocity is flattening steadily with the increment of positive value of 2nd order slip whereas the inverse trend is seen for temperature profile.

7. Declaration

The author(s) declared no potential conflicts of interest with respect to the research.

References

[1] J. Boyd, L. M. Buick, and S. Green, Phys. Fluids **19**, 093103 (2007).
[2] M. Mustafa, T. Hayat, I. Pop, and A. Aziz, Heat Trans. Asi. Res. **40**, 6 (2011).
[3] S. Nadeem, R. Mehmood, and N. S. Akbar, Int. J. Therm. Sci. **78**, 90 (2014).
[4] S. Rana, R. Mehmood, and N. S. Akbar, J. Mol. Liq. **222**, 1010 (2016).
[5] R. Ellahi, Appl. Mathema. Modelling **37**, 1415 (2013).
[6] S. Nadeem, S. Zaheer, and T. Fang, Numer. Algor. **57**, 2 (2011).
[7] C. Y. Wang, Int. J. Phys Fluids, **27**, 1915 (1984).
[8] L. J. Crane, Z. Angew. Math. Phys. **21**, 645 (1970).
[9] P. S. Gupta and A. S. Gupta, Can. J. Chem. Eng. **55**, 744 (1977).
[10] P. Carragher and L. J. Crane, Z. Angew. Math. Mech. **62**, 564 (1982).
[11] C. H. Chen, Heat Mass Trans. **33**, 5 (1998).
[12] H. I. Andersson, J. B. Aarseth, and B. S. Dandapat, Int. J. Heat Mass Trans. **43**, 1 (2000).
[13] S. Mukhopadhyay, Alex. Eng. J. **1** (2013).
[14] A. Ishak, R. Nazar, and I. Pop, Arabian J. Sci. Eng. **31** (2006).
[15] A. Ishak, Sains Malaysiana **40**, 4 (2011).
[16] T. Hayat, R. S. Saif, R. Ellahi, T. Muhammad, and B. Ahmad, Res. Phys. **7**, 765 (2017).
[17] K. B. Pavlov, Magnitnaya Gidrodinamika **10**, 4 (1974).
[18] V. P. Andersson, Acta Mechanica **95**, 1 (1992).
[19] T. Fang, J. Zhang, and S. Yao, Commun. Nonlinear Sci. Numer. Simul **14**, 7 (2009).

[20] M. Turkyilmazoglu, Int. J. Mech. Sci. **53**, 10 (2011).
[21] M. M. Bhatti, M. A. Abbas, and M. M. Rashidi, Appl. Math. Comput. **316**, 381 (2018).
[22] M. A. M. Faudzi, A. S. A. Aziz, and Z. M. Ali, In AIP Conf. Proc. **1974**, 1 (2018).
[23] E. M. A. Elbashbeshy, Arch. Mech. **53**, 6 (2001).
[24] S. Nadeem, T. Hayat, M. Y. Malik, and S. A. Rajput, Z. Naturforsch. **65a**, 495 (2010).
[25] F. Mabood, W. A. Khan, and A. M. Ismail, J. King Saud Uni. Engin. Sci. **29**, 1 (2007).
[26] M. Turkyilmazoglu, Commun. Nonlinear Sci. Numer. Simul. **63**, 373 (2018).
[27] J. Zhu, L. Zheng, and X. Zhang, J. Mech. Sci. Technol. **25**, 7 (2011).
[28] M. Gal-el-Hak, Trans. ASME J. Fluids Eng. **121**, 1 (1999).
[29] V. P. Shidlovskiy, Ameri. Elsev. Publis. Company Inc. New York, (1967).
[30] A. Majeed, A. Zeeshan, and R. S. R. Gorla, J. Natl. Sci. Found. **46**, 3 (2018).
[31] A. Yoshimura and R. K. Pridhomme, J. Rheol. **32**, 1 (1988).
[32] L. Wu, Appl. Phys. Lett. **93**, 25 (2008).
[33] S. Fukui and R. Kaneto, J. Tribol. **112**, 1 (2008).
[34] M. M. Bhatti, T. Abbas, and M. M. Rashidi, J. Magn. **21**, 3 (2016).
[35] M. M. Bhatti and M. M. Rashidi, J. Mol. Liq. **221**, (2016).
[36] J. Qing, M. M. Bhatti, M. A. Abbas, M. M. Rashidi, and M. E. S. Ali, Entropy **18**, 123 (2016).
[37] P. D. Ariel, T. Hayat, and S. Asghar, Acta Mech. **187**, 1-4 (2006).
[38] A. Zeeshan, H. F. Ismael, M. A. Yousif, T. Mahmood, and S. U. Rahman, J. Magn. **23**, 4 (2018).
[39] A. Majeed, F. M. Noori, A. Zeeshan, T. Mahmood, S. U. Rehman, and I. Khan, Case Stud. Ther. Eng. **12**, 765 (2018).
[40] L. F. Shampine, I. Gladwell, and S. Thompson, Cambridge University Press (2003).